Sensing Accuracy of a Conical Scan CO_2 Horizon Sensor

R. WEISS*
Lockheed Missiles and Space Company Inc., Sunnyvale, Calif.

A hybrid computer simulation of a conical scan horizon sensor was performed using the 15 μm spectral band to establish a vertical reference in Earth orbit. The sensing errors were derived from an analog simulation of the sensor operating on digital representations of the Earth radiance as seen by the conical-scanning sensor. Simulated bolometer outputs are compared with flight measurements. The sensing errors are found to be functions of vehicle position and altitude in orbit, heading, and time of year. The error mechanism described applies to the operation of conical scanning sensors in Earth orbits up to 6000 naut miles. The results will be useful in analyzing performance of three-axis stabilized systems such as Nimbus, Space Test Programs and Mercury. Typical behavior of the pitch-and-roll sensing errors is described for a range of orbit inclinations. The sensing errors are represented by their spectral components which will be useful for representing sensor low-frequency noise over an orbit. The most significant conclusion of the study is that the method of electronic processing of scanning sensor waveshapes can produce errors in attitude determination larger than those caused by climatological variations.

Introduction

Historical Approaches to the Problem

MANY approaches have been taken to defining the adequacy of the CO_2 horizon of the Earth as a precision attitude reference. Each approach has been determined by the tools and data available at the time to the investigator and the results presented in the format determined by the requirements of the immediate problem.

One approach involves the generation of horizon radiance profiles as functions of altitude above a spherical Earth for given times and positions. These profiles utilize the physical laws of the upper atmosphere together with actual data derived from balloon-and rocket-sondes. The profiles are analyzed to determine the stability of a given property of the profile. This basic stability in turn determines the limit of horizon sensing accuracy for a sensor which operates using the locator.[1-4] Performance of a given horizon locator can be inferred from the performance of some measured atmospheric property such as the temperature at an altitude corresponding to the 10 millibar (mb) pressure region. Since these basic data are more available from regular and special meteorological soundings, some investigators have used them to infer the stability of the CO_2 horizon.[5,6]

Direct measurement of horizon radiance profiles in various spectral bands as part of numerous orbital, rocket probe and aircraft programs provides experimental verification of the validity of the synthesized profiles to within the resolution and location accuracy of the measurement systems (1.5–2.0 km). But even these results are single point verifications of horizon characteristics, and do not shed data on the systematic variations over the entire globe and over long time spans, nor on the sensing error behavior for sensors in Earth orbit.

Presented as Paper 70-1021 at the AIAA Guidance, Control and Flight Mechanics Conference, Santa Barbara, Calif., Aug. 17–19, 1970; submitted March 2, 1971; revision received March 27, 1972. This work was funded under numerous Air Force Contracts. The author acknowledges the help of W. G. Uplinger in generating horizon radiance profile and bolometer outputs, L. J. Mistretta for his modelling of the horizon sensor, T. C. Anderson and H. W. Anson for their mechanization of the analog simulation of the sensor, and L. L. Dike for his digital systems assistance.

Index categories: Spacecraft Attitude Dynamics and Control; Spacecraft Navigation, Guidance, and Flight-Path Control Systems; and Atmospheric, Space, and Oceanographic Sciences.

* Staff Engineer, Guidance and Control Systems. Associate Fellow AIAA.

Approach to the Problem

A hybrid (digital/analog) computer simulation was undertaken at Lockheed Missiles and Space Company to investigate Earth horizon sensing performance and to support flight data analyses. Figure 1 illustrates the approach taken. Atmospheric data in the form of mean temperature and density as a function of height above the Earth's surface were used in a Univac 1108 computer simulation of the Earth's mantle. The output of this simulation was a set of horizon radiance profiles which are functions of the geometric height above the Earth of the instantaneous instrument line of sight (tangent altitude). These synthesized profiles were used, together with a representation of the horizon sensor scanning geometry and characteristics, in a CDC 6400 digital computer program to obtain simulated sensor bolometer outputs for any given space vehicle ephemeris.

The bolometer outputs were then used as inputs to a complete analog simulation of the horizon sensor circuitry on a Comcor 5000 analog computer to derive a pitch and a roll sensing error for each given vehicle position in orbit. Sensing errors as functions of vehicle position for worst case altitudes were plotted, and harmonic analyses later performed to obtain information on the spectral content of the horizon sensing error of a conical scan sensor in Earth orbit.

Of primary concern in this study is the determination of the low-frequency, high-power spectral components of sensing error arising from orbit and horizon characteristics. The instrument error sources such as bolometer noise, circuitry drifts and dynamic response, and output ripple are not discussed since they contribute negligible errors at frequencies below 0.05 Hz. It is the low-frequency content that is of prime interest to both the attitude control system and navigation system designers.

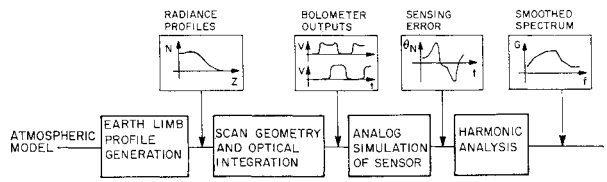

Fig. 1 Approach to the problem.

Conical Scan Horizon Sensor Operation

The horizon sensor comprises a pair of sensor heads and an electronics unit. The heads are mounted so that their optical axes slant down toward the horizon on opposite sides of the yaw axis in the plane defined by the pitch and yaw axes. It is assumed that the vehicle is oriented so that its yaw axis is coincident with the local vertical.

Each of the heads is designed so that its field of view (FOV) is offset from the scan axis and traces out a cone in space. In any given scan cycle (360° rotation of the FOV), each head detects the two basic radiation levels corresponding to Earth and space, with well-defined space-to-Earth and Earth-to-space transitions. The radiation profile so sensed is converted into a periodic two-level signal (bolometer output) processed in the electronics unit. The space-to-Earth transition will henceforth be referred to as the leading edge of the bolometer output wave, and the Earth-to-space transition as the trailing edge.

In addition to the radiance outputs, the heads each provide a scan phase reference output consisting of a train of spikes (index pulses) generated in synchronism with a fixed point (zero reference) in the scan.

The two-level bolometer signal must be converted into a square wave with well-defined leading and trailing edges. The basic circuit which performs this shaping is a differentiator/lag circuit called the "pipper" circuit. The positive and negative "pips", representing the space-to-Earth and Earth-to-space transitions, are thresholded at 50% of their peak values to form the leading and trailing edges of a square wave which is the shaped Earth pulse. The relative duty cycle (i.e., ratio of Earth pulse width to the total scan period) between the right and left head Earth pulses represents the roll attitude of the vehicle. The phasing of the Earth pulse with respect to the index pulse is a measure of vehicle pitch attitude.

In the configuration described, when the spacecraft is level with no roll or pitch error (solid Earth intercepts and wave shapes in Fig. 2), the heads sense equivalent amounts of Earth in any pair of corresponding scan cycles, and the duty cycle is the same for both radiance signals. Duty cycle, and not pulse width, contains the attitude information. In general, unless the two heads are scanning at exactly the same rate, the pulse widths will be different. The Earth portion of the scan cycle being generated by each head is symmetrically spaced about the zero reference for that head, and the radiation signals are thus in phase with the respective reference signals.

When the vehicle exhibits a roll attitude angle (dashed intercepts and wave shapes in Part A of Fig. 2), the two Earth/space ratios differ from each other by an amount proportional to the magnitude of the attitude angle. This difference produces a corresponding inequality in the duty cycles of the two radiance signals. The sense of the attitude (clockwise or counterclockwise) determines which of the two duty cycles is the larger. Despite the difference in duty cycle, as long as no pitch angle exists the Earth pulses from both heads are still centered about their respective index pulses.

When the vehicle exhibits a pitch attitude angle (dashed intercepts and wave shapes in Part B of Fig. 2), the Earth portion of each scan cycle is displaced with respect to the associated index pulse by an amount proportional to the magnitude of the error, and in a direction (leading or lagging) determined by the sense of the attitude. This displacement produces a corresponding shift in the phase relationship between the Earth and index pulses in each of the heads. As long as there is no concurring roll attitude, the duty cycles of the two radiance signals remain the same.

The accuracy of attitude sensing using the Earth's limb as a reference is a result of the interaction of the sensing instrument with the horizon properties. For the sensing concept described, any factor which can change the location of either the leading edge or the trailing edge of the Earth pulse is a source of horizon sensing attitude error.

Hybrid Simulation

Radiance Profiles

The radiance due to the Earth's atmosphere as seen from a point outside the atmosphere is calculated by numerically integrating the radiance and the transmission of each element of atmosphere along a given line of sight. This line of sight is the refracted optical path from the sensor through the atmosphere, becoming parallel to the Earth's surface at some point. The radiance calculation is performed for each of a number of wave-lengths spanning the 14–16 μm band. The radiation received by a given sensor is found by integrating with respect to wavelength for the filter function corresponding to the sensor optics. This filter function is based upon measurements performed by the horizon sensor manufacturer, and includes the spectral characteristics of the bolometer. The radiance thus found, when plotted as a function of tangent altitude, forms the radiance profile for the given latitude and month of the year. Two typical profiles are shown as Fig. 3. These profiles were calculated using mean measured atmospheric data for the two latitudes shown. Note the limb brightening evident in the equatorial profile. The extent in altitude of this brightening is approximately 30 km.

The general characteristics of the plot of peak radiance vs Earth latitude (Fig. 4) are significant in understanding the error behavior of the sensor. The winter radiance is lowest near the pole (0.85 w/m^2-sterad), and it remains relatively constant until about 70°N lat, at which point it increases rapidly. This rapid change over the mid-latitudes ends at

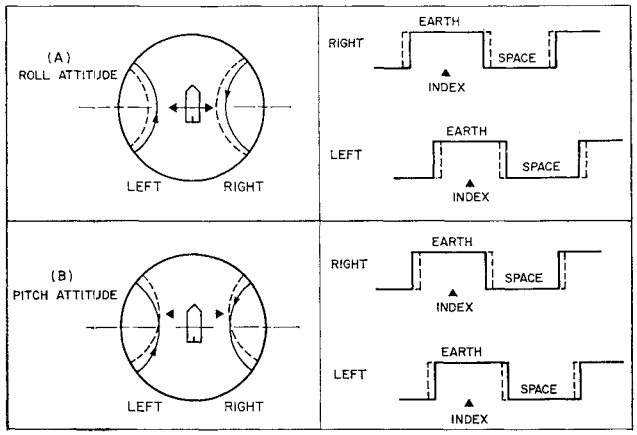

Fig. 2 Scan geometry and Earth pulses.

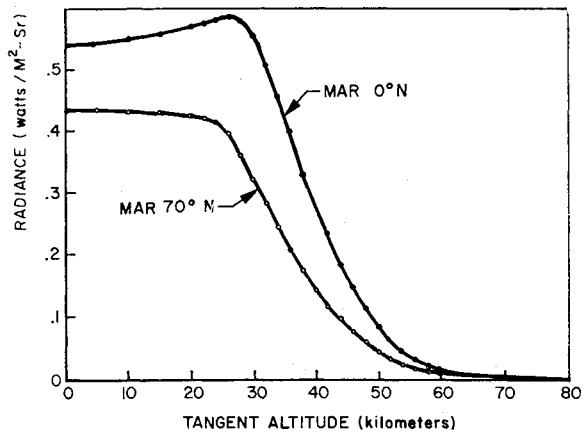

Fig. 3 Limb radiance for sensor optics.

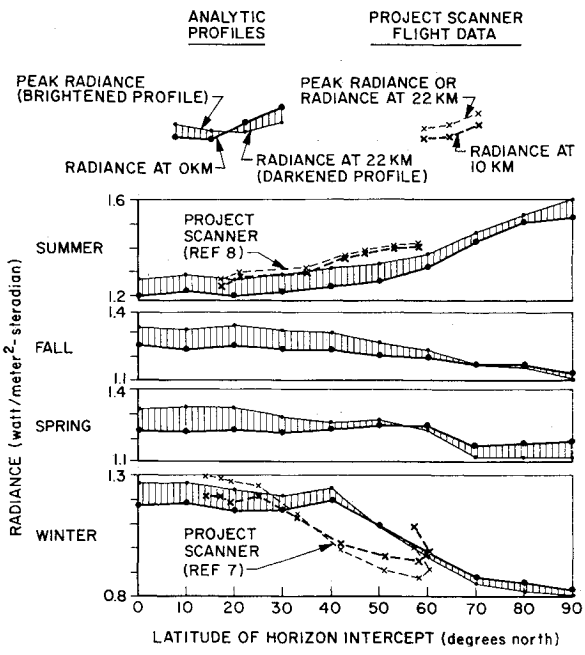

Fig. 4 Latitudinal behavior of radiance.

about 40°N lat, at which point the radiance takes on the moderate values associated with the equatorial region. Similar behavior occurs in the summer with the radiance levels increasing rapidly in the mid-latitudes and reaching a peak of 1.60 w/m²-sterad at the polar region. Plots made from Project Scanner profiles for a winter and a summer flight[7,8] show similar characteristics to the synthesized profiles both in their limb brightening/limb darkening behavior, as well as their radiance behavior with Earth latitude. It is shown later that the latitudinal variations in limb radiance, when seen by a scanning sensor, give rise to large sensing errors.

Of great significance in this study are the spatial correlation coefficients of horizon climatological variations. These will give a measure of correlation to be expected between the four horizon-crossing locations. It is of little consequence if the standard deviations of limb parameters are large when the spatial correlation between horizon-crossing locations is high. Using 10 mb temperature correlation coefficients as an indication of limb parameter correlation coefficients, the effect of climatological statistics on horizon-sensing accuracy can be estimated. This is a reasonable assumption because 30 km temperatures are a good estimate of located altitude conditions (Table 7, Ref. 4).

The 10 mb spatial correlation coefficients vary with both latitude and season. These coefficients have been tabulated for each month of the year as functions of latitude.[9] For all months, correlation is higher at the high latitudes than in the equatorial region. Correlation is highest, over-all, in the month of January, representative of the winter season. Consideration of the correlation coefficients for separation distances corresponding to the leading-to-trailing edge separation of one head, and to the left head-to-right head intercept separation, leads to an understanding of the effects of random horizon variations on the horizon sensor pitch and roll outputs.

It is shown[2] that the standard deviation of 10 mb temperature is highest during winter and at high latitudes. The fortuitous condition exists that those conditions (winter and high latitude) which lead to large variability of atmospheric properties also lead to high correlations of those properties between sensed horizon points. Therefore, sensing errors due to random climatological variation are reduced and the mean limb radiance profiles are a sufficient description of the horizon to calculate sensing errors resulting from differences in limb radiance profiles.

The previously mentioned spatial correlation is accounted for in the simulation by the modelling of the altitude and latitude of the horizon intercept during each scan cycle, and the use of the appropriate latitude-dependent radiance profile to compute the instantaneous bolometer output.

Bolometer Outputs

At each of 360 points along the scan, the output voltage of the horizon scanner detector is calculated by integrating the radiation over the instantaneous bolometer field of view. The measured transmission characteristic of the sensor lens system as a function of angle off the center of the FOV is modeled, and is convolved with the radiance surface to determine the total energy seen by the bolometer at that instant of time. This array of data points represents the bolometer voltage time history as each sensor head FOV scans through a complete scan cycle. Some typical Earth pulses are shown in Fig. 5, with scaled instantaneous bolometer output plotted against scan angular advance in degrees from the zero reference point.

The scan rotation of each FOV is counterclockwise, giving a leading-edge intercept for the right head FOV which is forward of the vehicle, and a trailing-edge intercept aft of the vehicle. The opposite is true of the left head FOV, i.e., trailing edge is forward and leading edge is aft. As the field of view sweeps through the atmosphere and across the Earth, the radiance seen by the bolometer is at each point predominantly a function of the latitude and altitude of the line of sight tangent point. It is possible to have considerable separation in the latitudes of the four intercepts for any given vehicle position and attitude.

Furthermore, the latitude of the tangent point will vary continually during each scan producing, in a worst case, a bolometer output as shown in Fig. 5C. The "horns" seen in this figure resemble in shape the phenomena of limb brightening observable in equatorial radiance profiles (Fig. 3), but are much more extensive, and are caused by the scanning of the FOV over a range of latitudes. This effect will therefore be called "scan-induced brightening" and will be distinguished from the "limb brightening" noted extensively in the literature.

The effect of limb brightening is minimized by the integration of the radiance over the sensor instantaneous FOV, and its full amplitude is not seen at the bolometer. See, for example, Fig. 3 where limb brightening is present only over a 30 km altitude region. On the other hand, the FOV extends over only 0.215° of Earth central angle (latitude), but is scanned over 8.4°. No attenuation of the radiance gradient due to scanning over latitude occurs as it does in scanning over the limb-brightened radiance profile.

Simulated Earth pulses were compared with the telemetered outputs for some selected cases. The bolometer output was conditioned in flight by a signal conditioner with a unity

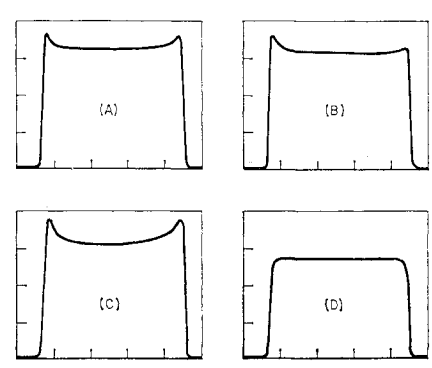

Fig. 5 Typical Earth pulses showing error-producing features.

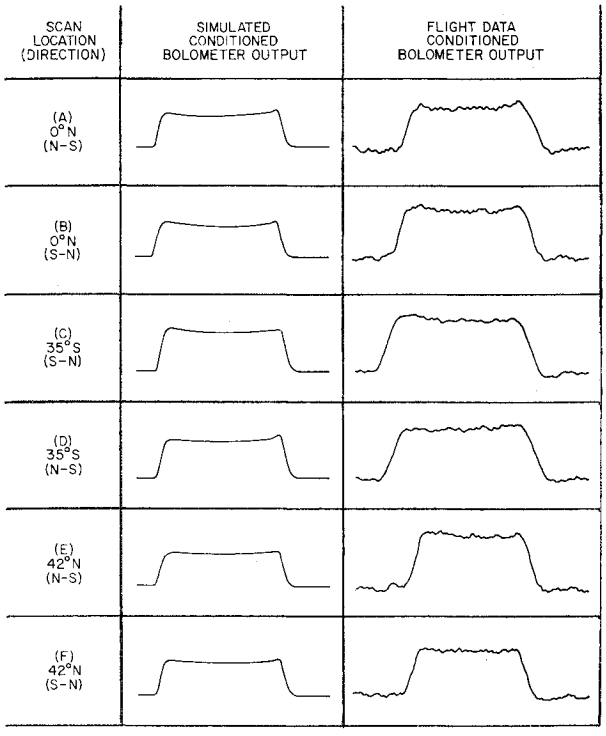

Fig. 6 Conditioned bolometer wave shapes December/January.

response at the scan frequency and with a first cutoff at 160 Hz. Furthermore, the conditioned signal was telemetered to the ground on IRIG Channel 8, with a 45 Hz bandwidth. In ground processing, a non standard filter was used to re-emphasize the high frequencies and recapture some of the lost edge information. The simulation includes the effects of the signal conditioning circuitry, but neglects the effects of the telemetry filtering. The general features of the conditioned bolometer wave shapes (Fig. 6) included varying amounts of leading and trailing edge brightening and leading-to-trailing edge tapering. A wave-by-wave comparison shows some preservation of these features and comprises a general verification of the horizon radiance modeling process. Note the relatively significant brightening in traces A and B, the negative and positive tapering in C and D, and the relatively flat Earth waves of E and F.

The major sensing error arises in the processing of the Earth pulse generated by the bolometer if that pulse shape is not ideal. Chief among the bolometer wave imperfections which induce sensing error for this particular processing method is a nonconstant radiance across the top of the Earth pulse, caused predominantly by the conical scanning motion through the limb and across the earth disc (scan-induced brightening). These errors appear as pitch-and-roll sensing errors resulting from processed earth pulses which exhibit incorrect length and phasing.

Passing a perfect trapezoidal bolometer pulse through the pipper circuits effectively differentiates the pulse, producing a positive pip corresponding to the leading edge of the earth pulse and a negative pip corresponding to its trailing edge. The clamp circuit following detects the point at which the differentiated waveform has a value of 50% of its peak value, and this point triggers a one-shot multivibrator which defines the leading edge of the located Earth pulse. If the Earth pulse has a flat top, then the differentiated wave goes to a zero value before the occurrence of the trailing edge pip, and the operation described previously is repeated for that edge. If, on the other hand, the bolometer output slopes between leading and trailing edges (Fig. 6D), then the pipper circuit differentiates that slope, and the trailing edge pulse starts from a nonzero level. For a negative taper (Fig. 6C) (radiance decreasing from leading to trailing edge) or for scan-induced darkening (Fig. 5D), an early trailing edge is defined by the threshold circuit, producing a shorter-than-desired processed Earth pulse whose center is advanced in phase from the reference pulse. This would give rise, for example, if it occurred on the right head, to negative roll and pitch indications. Scan-induced brightening and positive tapering (Figs. 5C and 6D), when they occur at the trailing edge of the processed Earth pulse, would cause errors in pitch and roll of the opposite polarity.

Simulated Performance in Earth Orbit

The simulated sensor was "flown" over various prograde and retrograde orbits to determine sensing error behavior in pitch and roll. Earth rotation and longitudinal horizon variations are not included in the simulation. The bulk of the cases were run for the worst month (January), which exhibits the greatest radiance variations for the Northern Hemisphere. Lack of adequate Southern Hemisphere meteorological data for the upper atmosphere prevented use of these profiles in the simulation. Symmetry was assumed for the Southern Hemisphere using the Northern Hemisphere radiance profiles displaced 6 months.

The cases were run in 10° and 15° increments of vehicle advance from the ascending node with the simulated vehicle in straight and level flight. Each case defines a pitch and a roll sensor output as the vehicle is "stopped" and the sensor scans repetitively across the Earth/space boundary at four points. There is no random noise generated in the simulation either in the horizon or in the sensor. These, perhaps, should be attempted in future studies involving the hybrid simulation.

Pitch-Sensing Error

Pitch error in winter is shown as a function of vehicle position in orbit in Fig. 7. For both the prograde and the retrograde orbits, maximum errors occur in the mid-latitudes where the radiance gradient with latitude is maximum, and can reach peak-to-peak magnitudes over one orbit of over 0.3°. The positive error maxima occur for all orbits on the northbound part of the winter orbit in the Northern and the Southern Hemispheres, and are caused by the relative geometry of the scan motion and radiance gradient which produces scan-induced brightening and darkening on the trailing edges of the bolometer waves.

Between the inclinations of 60° and 120° both heads are at some point in the orbit effected by the mid-latitude radiance gradient. Within this range of inclinations the pitch error over the winter portion of the orbit exhibits a bias which is a linear function of inclination. At 60°-inclined orbits, this bias is approximately +0.06°, and for 120°-inclined orbits the bias is −0.06°. The standard deviation of pitch error

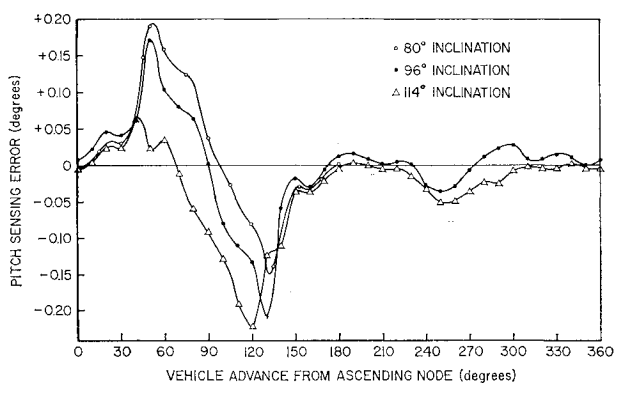

Fig. 7 Pitch-sensing error for various orbit inclinations (January).

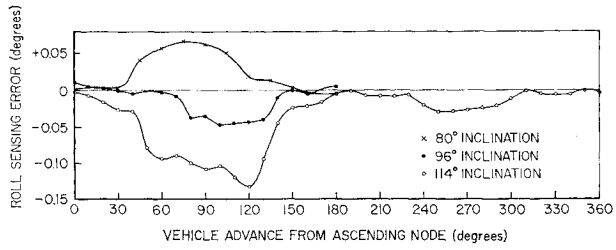

Fig. 8 Roll sensing error for various orbit inclinations (January).

over this range of inclinations is a very mild function of inclination, and ranges between 0.082° and 0.102°, with the maximum for the 90° orbit. Outside the 60–120° range of orbit inclinations, pitch-and-roll sensing errors decrease, because neither head can scan close to perpendicular to the radiance gradient and thereby produce the full effect of the scan-induced behavior.

Pitch-sensing errors are small in the equatorial region because of the cancelling effect of the errors of the right and left heads and because of the small radiance gradient in that region.

Roll-Sensing Error

The roll-sensing error with vehicle position over half an orbit is unidirectional (Fig. 8), as opposed to the pitch error which was shown to alternate polarity over the winter hemisphere. The mean roll error over half the orbit was found to be comparable to the pitch mean, and exhibits the same variation with orbit inclination. The roll standard deviation is considerably smaller than that of pitch. Again considering orbits with inclinations ranging from 60° to 120° the roll standard deviation is a maximum of 0.06° at inclinations 60° and 120°, and is a minimum of 0.015° for a polar orbit. The roll error standard deviation at orbits between increases linearly with the deviation of orbit inclination from polar. Again, at inclinations less than 60° and greater than 120°, both the mean and standard deviation of sensing error decrease rapidly.

Harmonic Analysis

A Fourier series expansion was made of the discrete time wave represented by the hybrid outputs for orbit inclinations of 96° and 114°. The results of the expansion indicate that the spectral content of the sensing error over a repeating orbit may be adequately described by the coefficients of the first four terms of the expansion.

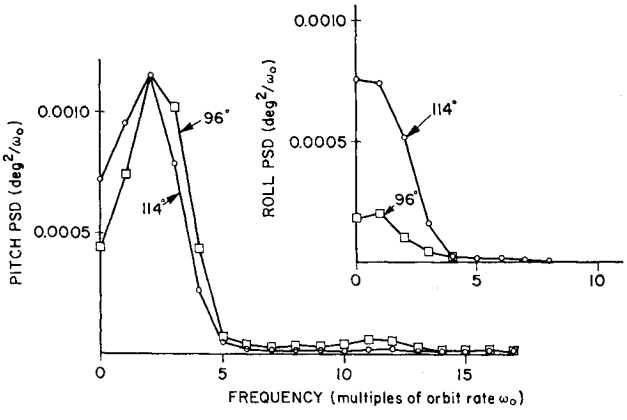

Fig. 9 Smoothed power spectra—sensing errors for two inclinations in January.

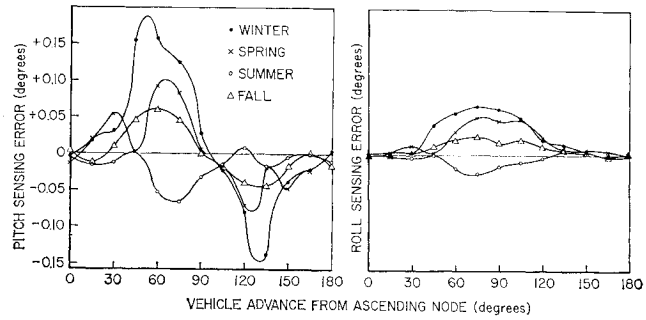

Fig. 10 Sensing error for four seasons (80°-inclined orbit).

Taking the Fourier components of the hybrid orbit performance runs, squaring each one and dividing by two results in the rms power contributed at each discrete frequency $n\omega_0$. Plotting this power against $n\omega_0$ yields the discrete or line spectrum for those hybrid runs. Smoothing the spectrum by applying Hanning weights to each component results in the smoothed spectra shown in Fig. 9. These spectra contain a concentration of power around $2\omega_0$ for pitch and ω_0 for roll, with very little power contributed by components beyond $4\omega_0$. This indicates that the power spectrum of seasonal horizon sensing error can be adequately represented by its frequency components below 5 times orbit rate. The next higher frequency components are not expected until about 50 times orbit rate, where the sensing error power contributed by local stratospheric anomalies would appear. And the highest frequency of interest would be the higher frequencies associated with instrument noise. But the investigation of these higher frequency sources is beyond the scope of this study.

Seasonal Variations

An intermediate orbit of 80° inclination was used to determine the effects of season on the roll-and-pitch error behavior (Fig. 10). The runs were confined to the orbit position interval of 0–180°. Winter errors are worst in pitch and roll due to the higher radiance/altitude gradient. The mean summer errors are of opposite polarity to those of winter, and the magnitudes of the standard deviations are from 3–4 times smaller. Spring and fall sensing errors are intermediate and no trend was determined in their means and standard deviations.

Hybrid Simulation Accuracy

The major source of error in the hybrid computer simulation are the radiance profile resolution, analog-to-digital conversion resolution, run-to-run stability, and the effect of noise on the analog processing circuitry. In addition, there is a day-to-day run stability due to the accuracy of the automatic potentiometer-setting servos. Over-all accuracy of the simulation appears to be about $\pm 0.01°$, based on the use of test cases interspersed between the batches of production cases.

Summary of Results

Pitch-and-roll sensing errors on orbit may be as high as $\pm 0.22°$ for Earth orbiting conical scan sensors of the type studied. These errors are functions of season, altitude, position in orbit, and vehicle attitude. For any given orbit mean pitch or roll errors can exist over the entire orbit because of the sensing geometry. The major part of the error power is at the lower frequencies, from orbit rate to 4 times orbit rate. Rms errors over all orbits studied were 0.11° or less.

The major horizon sensing error source was found to be due to the method of signal processing of bolometer outputs which are not flat over the Earth pulse. These radiance variations over the Earth pulse are due predominantly to the geometry of scanning over a range of latitudes where radiance is not uniform. The effects of uniformly tapered or sloping Earth pulses, previously thought to be the chief error contributors, seem to be not as severe as the effects near the pulse edges of the scanning over different latitudes. For a conical scan sensor of the type studied, errors due to scan-induced brightening are larger than the expected errors due to climatological variations, and the greatest accuracy improvements at this time will result from an optimization of the pulse processing.

References

[1] Bates, J. C. and Jensen, C. A., "Horizon Definition Study Summary," NASA CR-66432, May 1967, Honeywell Inc., Minneapolis, Minn.

[2] Bradfield, L. G. and Nelson, G. D., "Located Horizon Variation Study Final Report," NASA CR-66748, Jan. 1969, Honeywell Inc., Minneapolis, Minn.

[3] Burn, J. W., Uplinger, W. G., and Morris, P. P., "Earth Limb Radiance Profiles for the 15-Micron Carbon Dioxide Absorption Band," LMSC-677317, March 1967, Lockheed Missiles and Space Co., Sunnyvale, Calif.

[4] Thomas, J. R., "Derivation and Statistical Comparison of Various Analytical Techniques Which Define the Location of Reference Horizons in the Earth's Horizon Radiance Profile," NASA CR-726, April 1967, Honeywell Inc., Minneapolis, Minn.

[5] McArthur, W. G., "Horizon Sensor Navigation Errors Resulting from Statistical Variations in the CO_2 14-16 Micron Radiation Band," *Transactions of the 9th Symposium on Ballistic Missiles and Space Technology*, Vol. 1, Aug. 1964, U.S. Naval Training Center, San Diego, Calif., pp. 261–289.

[6] Patterson, C. L., "Error Sources in Earth Horizon Sensing," M. S. thesis, 1967, Univ. of California, Los Angeles, Calif.

[7] Whitman, R. I., McKee, T. B., and Davis, R. E., "Infrared Horizon Profiles for Winter Conditions from Project Scanner," TN-D-4905, Dec. 1968, NASA Langley Research Center, Hampton, Va.

[8] McKee, T. B., Whitman, R. I., and Davis, R. E., "Infrared Horizon Profiles for Summer Conditions from Project Scanner," TN-D-4741, Aug. 1968, NASA Langley Research Center, Va.

[9] Staff, "Temperature Characteristics at 30 Kilometers," Rep. 5501, July 1966, USAF Environmental Technical Applications Center, Washington, D. C.